METROLOGY AND MEASUREMENT SYSTEMS

Index 330930, ISSN 0860-8229

www.metrology.pg.gda.pl

FAST ESTIMATION OF THE NON-STATIONARY AMPLITUDE OF A HARMONICALLY DISTORTED SIGNAL USING A KALMAN FILTER

Uroš Kovač[1], Andrej Košir[2]

1) Metrel d.d., Ljubljanska cesta 77, 1354 Horjul, Slovenia (✉ uros.kovac@metrel.si, +38 64 027 7224)
2) University of Ljubljana, Faculty of Electrical Engineering, Tržaška cesta 25, 1000 Ljubljana, Slovenia (andrej.kosir@fe.uni-lj.si)

Abstract

In this paper we introduce a self-tuning Kalman filter for fast time-domain amplitude estimation of noisy harmonic signals with non-stationary amplitude and harmonic distortion, which is the problem of a contact-voltage measurement to which we apply the proposed method. The research method is based on the self-tuning of the Kalman filter's dropping-off behavior. The optimal performance (in terms of accuracy and fast response) is achieved by detecting the jump of the amplitude based on statistical tests of the innovation vector of the Kalman filter and reacting to this jump by adjusting the values of the covariance matrix of the state vector. The method's optimal configuration of the parameters was chosen using a statistical power analysis. Experimental results show that the proposed method outperforms competing methods in terms of speed and accuracy of the jump detection and amplitude estimation.

Keywords: amplitude estimation, harmonic signal, harmonic distortion, Kalman filter.

1. Introduction

Digital signal processing is an important branch of electronic measurement technology. The measurement of parameters of harmonic signals is one of the most important tasks. Due to the nature of the measurement of grounding resistance, contact-voltage measurements, line-resistance measurements, RCD (residual-current device) test measurements [1], the frequency and phase of the harmonic signal are known in advance and the only parameter that needs to be estimated is the amplitude. The problem of a fast (in terms of a signal period) non-stationary amplitude estimation with harmonic distortion can be solved by using a self-tuning, multi-frequency, Kalman filter (KF) model, based on an observation of the innovation vector.

Currently, the field of measurement technology mainly uses non-iterative methods for the amplitude estimation of harmonic signals, *e.g.*, fast Fourier transform (FFT) based methods [2], digital filters (FIR or IIR) [3–6] root-mean-square (RMS), least squares, weighted least squares, filterbank approaches, *etc*. [6]. The inability to adapt to changes in the sampled signal is the drawback of the non-iterative methods. This is one of the reasons why we selected the KF-based method. Other reasons are favorable statistical properties of KF's internal variables for the moment of amplitude jump detection. Promising results in different areas of research and the ability to expand the model to higher harmonics encouraged us in this choice of adaptive methods.

Since the objectives of the proposed method are fast detection of the moment of the amplitude jump and fast, accurate amplitude estimation, we believe our method cannot be compared to Fourier transform (FT) and spectrum based methods in a fair way. The problem of such comparison is the determination of the observation time window length. If the time window for FT is chosen to be one whole period long, the moment of jump detection

cannot be fast. On the other hand, if a short time window (below one period) is used, the amplitude estimation is not accurate enough.

The comparison with RMS based methods is not feasible in a fair way as well. The restriction of the time window length to one, one half or one quarter of the period does not allow fast detection of the amplitude jump. Using other sub-period interval lengths requires a known signal phase in order for the amplitude to be estimated using the RMS formula.

The comparison of the proposed method to classic adaptive methods such as presented in [7] could be done but we omit it and postpone it until further work. Such a comparison would require a whole new research to be carried out to develop a fast and accurate amplitude jump estimation adaptive method. The potential of such method is difficult to assess, especially in terms of fast amplitude-jump detection.

Therefore, the proposed method is compared with a single frequency KF based method only. The performance of a single frequency KF based method compared to competitive ones will be published in a parallel research work.

The choice of the KF model was made between the linear (*e.g.*, [8]) and the extended (*e.g.*, [9–10]) KF models. Since we were tracking changes in the amplitude, we needed a method that is one-step transition-linear without error. By adding higher harmonic components of the signal in the model, we created an exact transition model so that the error detected in the innovation vector was directly connected with the measurement noise and the change of parameters and did not include the error of the rounded estimation, as it does in the extended KF models. More details about the selected KF model can be found in Section 2.

1.1. Related work

The Kalman filter (KF) has been used for many problems in the past. Here, we present the selected KF-based researches in the field of a non-stationary amplitude of harmonic signals that encouraged us to develop our method. In [11] the problem of a non-stationary amplitude estimation of a harmonic signal with harmonic distortion is addressed with a test of the auto covariance of the innovation vector. A statistical test is used to detect the jump, which triggers the correction of the covariance matrix of the state vector to high predefined values. In [14] the detector of the jump is based on the observation of the difference between consecutive samples of the signal. Detection is executed by a statistical test on previously processed samples of the signal at every iteration. In [16] a loop is executed for every sample that corrects the covariance matrix of the excitation vector and the Kalman gain with a comparison of the a-posteriori and a-priori estimates of the state vector. An extended, real, Kalman-filter model is proposed for a time-varying harmonics estimation in [14]. When the extended Kalman filter is used, the transition between steps is not linear without error. Consequently the information of an amplitude jump cannot be extracted from the innovation vector, which is no longer directly correlated to measurement noise of the signal. This is also the main reason why we chose a linear KF model.

1.2. Problem statement

The aim of our research was to solve the problem of fast detection of the amplitude jump and accurate estimation of the non-stationary amplitude of noisy harmonic signals with added higher harmonic components. The term *fast* refers to the time interval in which the analyzed samples are taken being as short as possible; typically only a fraction of the signal period. The main issues of this problem are as follows: 1. fast detection of the moment of the amplitude jump, 2. response to this jump in the Kalman filter (KF) internal states (in phase space)

by resetting the covariance matrix of the state vector, and 3. the speed of convergence of the estimated amplitude after the jump of amplitude for short sub-period stationary signals.

In researches mentioned before in Section 1.1. we identified the following drawbacks, which we tried to overcome. First is the undefined length of the observed window of a selected Kalman filter variable – we solve this problem with statistical power analysis and control of type I error. The next problem was the reset of the covariance matrix used after the detection of the amplitude jump – we use the values of the variance of the innovation vector in order to adapt to the size of the amplitude jump. Finally, the problem of used loop in [16] is addressed by using a statistical test on the observed window, since the loop for every sample prolongs the execution time of the method and makes it variable and difficult to predict.

This paper is organized as follows. The introduction is followed by a section in which we present the measurement and theoretical background of our research. This is followed by a description of the proposed method and materials and methods used in our experiments. Finally we present results and give a discussion on obtained results. At the end of the paper a conclusion with plans for future work is given.

2. Measurement and theoretical background

2.1. Measurement background

The proposed method is applicable to different measurements, *e.g.*, in line-resistance measurements, in the tracking of harmonic fluctuations in power systems, *etc*. Nevertheless, we introduce our method for the contact voltage measurement because of its simplicity in terms of understanding. The contact voltage is the voltage that can occur as a result of fault conditions of the earthing resistance on any conductive, accessible parts that can come into contact with the human body. The value of the maximally allowed contact voltage is called the limit voltage and is usually 50 V, although in some cases (hospitals, computer rooms, rural environment, *etc*.) it is just 25 V [12].

Normally, the contact voltage is equal to the difference between the voltage when the circuit under test is loaded (loaded voltage) and the voltage when the circuit under test is not loaded (unloaded voltage). The test instrument simulates a fault current that is driven from the phase conductor to the protection conductor and then to ground. The test current starts at low values (*e.g.*, 5 mA) where the loaded voltage is measured (Fig. 1). The unloaded voltage is also measured. If the difference between the loaded and the unloaded voltage is within predefined safety levels, the test current is increased and the loaded and unloaded voltages are measured again. If possible this procedure is repeated up to a test current of half of the nominal tripping current of the installed residual-current device (RCD). The difference in the measured voltages is upscaled to the nominal tripping current. If this difference in the voltages is lower than the limit voltage (25 V or 50 V) the earthing resistance is low enough and thus the contact voltage is within the declared boundaries for safe use [13].
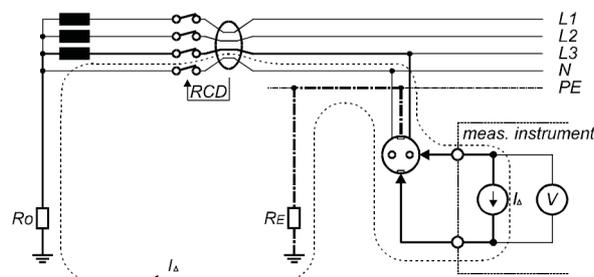

Fig. 1. Principle of a contact-voltage measurement.

During the measurement of the contact voltage the instrument successively drives a test current (loaded signal) in short intervals. However, because of slow disturbances on the power supply the loaded and unloaded signals must be close together, and therefore a fast and accurate estimation of the amplitude is of crucial importance. Also, because the measurements are taken on the (loaded or unloaded) power-supply network, the higher harmonic components are added to the measured signal, which reduces the accuracy of the observed fundamental component. The separation of harmonic components is necessary. Currently, with the use of FFT method, the interval length of the loaded and unloaded signals is one period (20 ms at 50 Hz), but we try to shorten this interval to sub-period signals in order to measure the loaded and unloaded signals as close together as possible. From each measured voltage signal (loaded and unloaded) the effective amplitude is computed with an FFT method. The difference in the amplitudes of the loaded and unloaded signals is then re-calculated into the contact voltage, depending on the test current used and the tripping current of the installed RCD device.

2.2. Theoretical background

2.2.1. Kalman filter

The base of the configuration of the KF for our method is described in [8], except that our configuration is extended to odd higher harmonics. This configuration follows from the derivation of cosine and sine as two state-vector variables and is presented as (1), (2):

$$\mathbf{x}[k+1] = \mathbf{F}[k]\mathbf{x}[k]$$
$$= diag(F_d[k,1], F_d[k,2], F_d[k,3], F_d[k,4]) \mathbf{x}[k], \tag{1}$$
$$F_d[k,i] = \begin{bmatrix} \cos([2i-1]\omega\Delta t) & \sin([2i-1]\omega\Delta t) \\ -\sin([2i-1]\omega\Delta t) & \cos([2i-1]\omega\Delta t) \end{bmatrix},$$

$$\mathbf{z}[k+1] = \mathbf{H}[k]\mathbf{x}[k+1] + \mathbf{v}[k+1]$$
$$= \begin{bmatrix} 1 & 0 & 1 & 0 & 1 & 0 & 1 & 0 \end{bmatrix}\mathbf{x}[k+1] + \mathbf{v}[k+1], \tag{2}$$

where $\mathbf{x}[k]$ is the state vector, $\mathbf{F}[k]$ is the transition matrix, $\mathbf{F_d}[k]$ is the partial diagonal transition matrix modeling one harmonic component, $\mathbf{z}[k]$ is the measured signal vector, $\mathbf{H}[k]$ is the measurement matrix and $\mathbf{v}[k]$ is the measurement noise vector. We decided to track three additional harmonic components according to the spectrum of signals produced by real measurements. However, the presented method is applicable to any reasonable low number of harmonic components. The excitation vector is omitted in the configuration of the used KF model as we do not use it to keep the one-step transition exactly linear. For our simulations we modeled the first three odd harmonic components as they tend to have the highest values and thus the highest impact on the distortion of the fundamental component. $\mathbf{F}[k]$ is the block diagonal as we assume that the dependence between harmonic components can be ignored with no significant loss of model efficiency and is thus omitted from the KF model.

With this configuration we track the real ($\mathbf{x}_{i,1}$) and imaginary ($\mathbf{x}_{i,2}$) components of the complex representation of a harmonic signal for the i-th modeled harmonic component. The state vector thus includes both time samples of the cosine and sine. With the state vector defined we can estimate the amplitude of the fundamental component (50 Hz) of the signal by applying (3) to the states of the fundamental component and thus estimate the amplitude of the fundamental component (50 Hz) of the signal at every step of the processing.

The procedure for the KF algorithm is shown in the following set of (4). The symbol "–" denotes a-priori estimates of the state vector and the covariance matrix of the state vector and **y** is the innovation vector that we use for statistical testing.

$$\hat{A}_1[k] = \sqrt{x_{1,1}^2[k] + x_{1,2}^2[k]}$$
$$= A_1 \sqrt{\cos^2(\omega\Delta tk + \phi) + \sin^2(\omega\Delta tk + \phi)} \tag{3}$$

$$\mathbf{x}^-[k+1] = \mathbf{F}[k+1]\mathbf{x}[k],$$
$$\mathbf{P}^-[k+1] = \mathbf{F}[k+1]\mathbf{P}[k]\mathbf{F}'[k+1],$$
$$\mathbf{y}[k+1] = \mathbf{z}[k+1] - \mathbf{H}[k+1]\mathbf{x}^-[k+1],$$
$$\mathbf{K}[k+1] = \mathbf{P}^-[k+1]\mathbf{H}[k+1]'(\mathbf{H}[k+1]\mathbf{P}^-[k+1]\mathbf{H}[k+1]' + \mathbf{R}[k+1])^{-1}, \tag{4}$$
$$\mathbf{x}[k+1] = \mathbf{x}^-[k+1] + \mathbf{K}[k+1]\mathbf{y}[k+1],$$
$$\mathbf{P}[k+1] = \mathbf{P}^-[k+1] - \mathbf{K}[k+1]\mathbf{H}[k+1]\mathbf{P}^-[k+1].$$

We detect the jump of the amplitude because of the property of the KF called drop-off. Drop-off is a phenomenon of a KF that occurs when the estimated parameter is stationary for a long time and thus the accuracy of the estimated parameter increases, but at the same time the sensitivity to changes in the estimated parameters decreases [11] (Fig. 2). As it can be observed in Fig. 2, the values of the covariance matrix of the state vector decrease rapidly in the stationary state and thus the confidence in the model increases. When the jump of the amplitude occurs (at $N/N_p = 1$), the deviation of the estimation of the amplitude from the model increases and because of that we have to artificially force the KF to have a higher confidence in the measurements and thus converge to a new amplitude of the signal. This involves resetting the covariance matrix of the state vector to higher values.
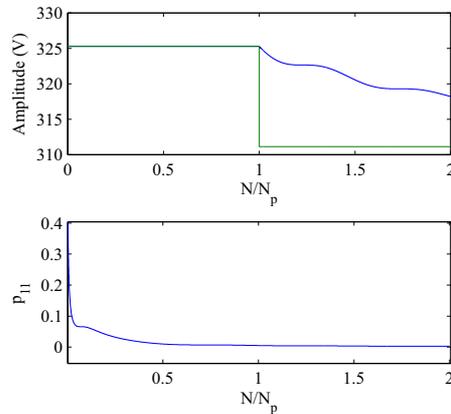

Fig. 2. Amplitude tracking and the first diagonal element of the covariance matrix of the state vector (p_{11}) at the drop-off is shown. The horizontal axes of the graphs represent the ratio between the number of the current sample (N) and the number of samples of one period (N_p).

We assume that the KF conditions for optimal use are met during the KF's steady state. These are as follows:
1. The measurement noise is white Gaussian noise;
2. The process noise is white Gaussian noise;
3. The measurement noise, process noise and measurement signal are uncorrelated.

If these conditions are met, the innovation vector of the KF in the steady state is white noise [17] and the jump occurrence disturbs the distribution of the innovation vector. These assumptions were verified with statistical significance tests of the innovation vector but are not reported in this paper.

2.2.2. Statistical properties of the Kalman filter variables

In this section we present statistical properties of the Kalman filter for a fast and accurate estimation of the non-stationary amplitude of a noisy harmonic signal with harmonic distortion. For self-tuning of the KF we use statistical hypothesis testing to detect the change in the amplitude, analysis of the KF internal states to identify the required values and control of multiple-hypothesis testing problem.

In [17] a general approach of statistical testing in the KF is presented, but the statistical power analysis for the optimal sample size is not considered. We used statistical power analyses to determine the optimal length of the observed window and, consequently, control both types of errors in the KF state transitions (jump detection and the end of the settling-time state detection).

Each cycle of the measurement is divided into three time consequential states or phases, (1) steady state before the amplitude change, (2) moment of the jump and (3) settling-time state (the time interval when the KF is converging to a new value of the amplitude), see Fig. 4. The next state is a new steady state that is a part of a new cycle. I_ϕ is the observed window of the innovation vector used for a statistical test of the KF state and I_σ is the window of the innovation vector used to compute the variance of the innovation vector in the steady state.

For this analysis the relevant aspects of the three listed states are:
1. Steady state: the accuracy of the estimated amplitude is high and the innovation vector represents the measurement noise if the KF optimality conditions are met.
2. Jump: the moment of the change of the amplitude value where the innovation vector is the sum of the measurement noise and the value of the jump. The trust in the estimated state of the KF must be lowered in order to allow the sudden change in the KF internal values.
3. Settling-time state: the time period after the jump is detected where the innovation vector is a sum of the measurement noise and the estimation error as the estimation has not yet converged towards the true value of the amplitude (excitation vector is zero).

A null hypothesis of the test of the jump of the amplitude occurring is H_0 = [KF is in the steady state at the step k]. Assuming H_0, the standardized squared Euclidean norm is taken as the proposed test statistics $\phi_j(\mathbf{y}, I_\phi(k,l)) = \left\| \mathbf{y}[k,l] \right\|_2^2 / \sigma_k^2$, which is distributed according to the $\chi^2(l)$ distribution since the innovation vector is white noise [17], σ_k^2 is an estimated variance of the innovation vector, $I_\phi(k,l) = \{k - l + 1, ..., k\}$ is the observed time window and $\left\| \mathbf{y}[k,l] \right\|$ is Euclidean norm ($\left\| \mathbf{y}[k,l] \right\|_2 = \sqrt{y_{k-l+1}^2 + ... + y_k^2}$). When the null hypothesis H_0 is rejected against the alternative hypotheses H_1 = [KF is not in the steady state at the step k], a jump is detected. Therefore, the detection condition is given by a critical value of the statistic $\phi_{j,cr}$ computed from the $\chi^2(l)$ distribution at the selected risk level α. To control the type I detection error the risk level $\alpha = 0.05$ was used and the observed window length was used to control the type II detection error.

The idea for detection of the end of the settling-time state is that we use the same test statistics ϕ to detect the KF step when the settling-time state ends and that we store the required statistical moments (variance in this case) from the observed window before the last

jump occurs. Because of the short observed window we assume that the measurement noise is stationary.

The problem of multiple hypotheses testing arises [18], since we apply hypotheses testing at every KF algorithm step. The occurrence of errors is inevitable: type I errors occur at rate α and type II errors occur at rate β, where *1-β* is the achieved (posteriori) power of the test. Our approach to mitigate a false phase-transition detection is to accept detection, not at the first statistical test identification, but only after several identifications (n_j times after the first rejection of the null hypotheses H_0 for the jump detection and n_s after the first acceptance of H_0 after the end of the settling-time state detection). This reason is based on the fact that when a given phase of the KF occurs it lasts for several steps and the detection procedure should detect it at most of the successive steps. The drawback of this approach is that it increases the reaction time of the phase-transition detector, which is of particular importance for jump detection since our goal is the fast detection of the amplitude change.

3. Proposed solution

In this section, we present the proposed solution for before mentioned problems of our research. First, we present the procedure of self-tuning Kalman filter for detection of states. Next, we determine the optimal length of the observed window and initial values of the Kalman filter. Finally, we give the procedure of determining the values of the covariance matrix of state vector at reset of the KF.

3.1. Proposed architecture of the self-tuning KF

The following steps are performed in the procedure for the KF state detection (see Fig. 3). First, at the beginning of the estimation, the KF is naturally in the settling-time state and the jump detector is switched off; at the end of the settling-time state the detector is switched on and the procedure of resetting the covariance matrix is started. After the first detection of the end of the settling-time state, the KF is set to the steady-state mode and the normal operation starts. When the jump is detected, the jump detector is switched off and the detector for the end of the settling-time state is switched on. The procedure of resetting the covariance matrix is started. These steps are then repeated in cycles.
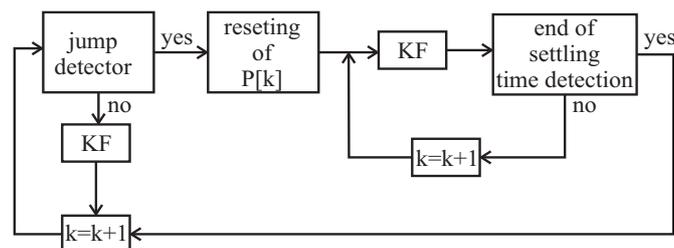

Fig. 3. Conceptual figure of the procedure of the KF-states' detection.

3.2. Window length determination

Typically, by presetting the lower bound of the a-priori power *1-β* the minimal length of the observed window ($l = diam(I_\phi)$ in our case) for a given effect size is determined [19, 20]. The required length of the observed window goes by the increased a-priori power. According to Fig. 4 this is not true with the proposed test for jump detection since the achieved (posteriori) power is reduced for longer observed windows. The reason is that at the time

moment of the jump detection, which is always detected after a certain detection delay Δt, the observed window I_ϕ is already partially in the time region where the alternative hypothesis H_1 is true, *i.e.*, $I_\phi = I_\phi |_{H_0} \cup I_\phi |_{H_1}$, see Fig. 5. Here, $I_\phi |_{H_0}$ is the part of the observed window restricted to hypothesis H_0 and $I_\phi |_{H_1}$ is the part of the observed restricted to hypothesis H_1. With a longer observed window, the ratio of the numbers of the observed samples $diam\left(I_\phi |_{H_0}\right) / diam\left(I_\phi |_{H_1}\right)$ is reduced and as a consequence the achieved power is reduced as well. Therefore, the lower limit on the observed window length l cannot be determined by a power analysis, but the upper limit can be what we use in the optimal KF configuration setting.
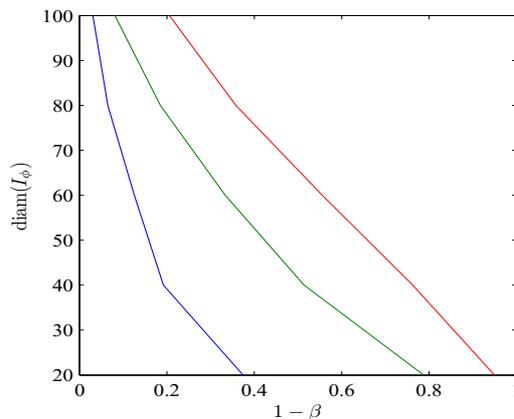

Fig. 4. Graph of the dependence of the observed window length $l = diam(I_\phi)$ on the power $1 - \beta$ (blue – delay is 5 samples, green – delay is 10 samples, red – delay is 15 samples).
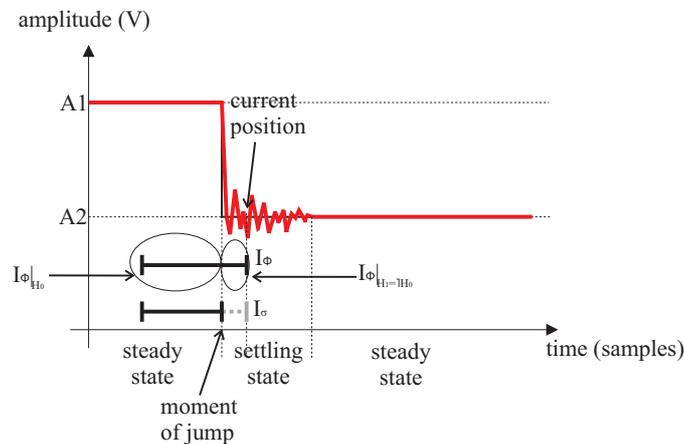

Fig. 5. Conceptual figure of the KF states with emphasis on the transition of the observed window for statistical testing from the steady state via the jump state to the settling-time state.

The question of how to select the lower limit $l = diam(I_\phi)$ arises naturally. According to Fig. 4, the shortest observed window is the best choice, which simply cannot be true. The answer follows from the construction of the statistical test itself. If the observed window l is too short, the assumption about the probability distribution of the test statistics ϕ, assuming the null hypothesis to be $\chi^2(l)$, is not valid any more. Consequently, the KF state-detection

procedure is stuck in false detections as the rate of the type I error goes up. This is particularly critical when the effect size (the size of the amplitude jump) is low. Therefore, we use the type I error control and small-sample-size statistical testing to determine the lower limit as $l = diam(I_\phi)$. The values depend on the measured signal characteristics, as reported in the results in Section 5.

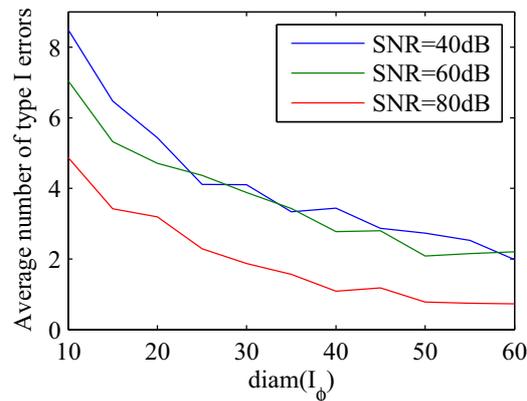Fig. 6. Graph of the dependence of the average number of type I errors at different observed window lengths $l = diam(I_\phi)$ for different regimes of tested signals (blue – SNR=40 dB, ΔA=10 V; green – SNR=60 dB, ΔA=10 V; red – SNR=80 dB, ΔA=10 V).

The results relating to type I error control for different signal-to-noise ratios (SNR) are presented in Fig. 6.

3.3. Setting the Kalman filter initial values

The use of the KF demands the initial values to be defined before the estimation starts. Those are the initial values of the state vector and its covariance matrix and the covariance matrix of the measurement noise. In our experiments we used the following definitions of these parameters.

The initial value of the state vector was set to $\mathbf{x}[0] = [0; 325; 0; 3.25; 0; 3.25; 0; 3.25]$ because we know that the amplitude of the fundamental sine component is near 325 V and the phase is zero at the beginning of the measurement (the nature of the measurement provides the conditions so that this is always true). Because the phases of the higher harmonic components are not known beforehand we set the initial values so that the computed amplitude of each component is equal to 1% of the fundamental component (as the simulated signal contains these components).

Next we had to establish the initial values of the covariance matrix of the state vector. The covariance matrix tells us how accurate the estimation of the state vectors is. At the beginning and at jumps the estimated state vectors are not very accurate as the KF has not yet converged. This is the reason why we selected relatively high values for the diagonal elements of the initial covariance matrix of the state vector (*e.g.*, 10**I**, **I** is the identity matrix). We also tested the effect of the initial value of the covariance matrix of the state vector on the relative error of the amplitude estimation and the results are shown in Fig. 7. The format of the initial covariance matrix for this test is the diagonal matrix $p\mathbf{I}$ and the parameter p is real non-negative. The results are given in Fig. 7. We observed that the relative error decreases with larger values of p and that is why we set the initial covariance matrix of the state

vector to high values. In this experiment the relative errors of the amplitude estimates with different initial covariance matrices are computed after 16 processed samples of the signal.
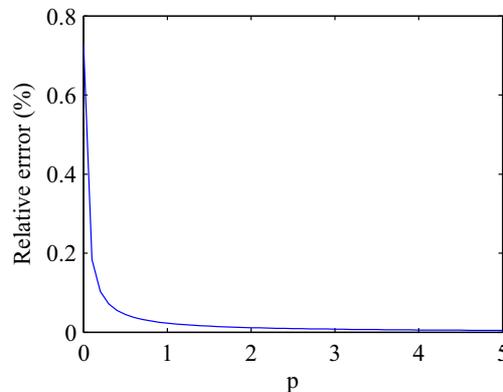

Fig. 7. Relative error of the amplitude estimates after 16 processed samples of signal depending on the parameter p of the diagonal covariance matrix ($\mathbf{P} = p\mathbf{I}$).

The last parameter of the KF model that had to be set was the covariance matrix of the noise. The only problem here is establishing the parameters of the noise. But with a knowledge of the reference signal and higher harmonic components we simply subtracted the measured signal with the harmonic signal and the result was the signal of added noise ($\mathbf{v}$), for which we estimated the covariance matrix using the equation $\mathbf{R} = \text{cov}(\mathbf{v})$. In real situations we believe that for a given class of signals the same initial matrix $\mathbf{R}$ is satisfactory.

3.4. Resetting of the KF after the amplitude jump

After the jump has been detected we reset the KF by replacing the current covariance matrix of the state vector with the identity matrix multiplied by the computed variance of the observed innovation vector window. The variance of the observed innovation vector at the jump is higher than the elements of the covariance matrix at the steady state and thus the sensitivity to change of the estimated amplitude is higher, *i.e.*, the dropping-off is avoided. On the other hand, if the jump is falsely detected the variance of the observed innovation vector is low and it does not cause a significant error in the steady-state amplitude estimation of the KF. Another issue for resetting the KF was the use of an identity matrix as a base for the reset. First, we used a matrix that only resets the fundamental harmonic component, as it is the only one that changes at the jump. But we observed that this kind of reset causes the innovation vector not to be correlated with the measurement noise anymore in the steady state and thus it is not employable for the detection of successive jumps. We discovered that the jump of the fundamental harmonic component inserts a small but wide spectrum of higher harmonics, which influences all the higher harmonics that we estimate. Therefore, we decided to use the identity matrix as a base for the reset matrix, as it turned out that in this case the innovation vector is correlated with measurement noise after the jump and is thus employable for the detection of the successive jumps. To sum up, in order to allow a fast change in the KF state space, immediately after the jump is detected we set the diagonal elements of the covariance matrix to higher values than those estimated by the KF algorithm. This allows us to guide the KF at the beginning of the settling-time state, firstly to accept a quick change and secondly to converge fast enough.

4. Materials and methods

In this section we present basic properties of both simulated and real signals under investigation. We also give the evaluation measures for comparison of obtained results with each method.

4.1. Evaluation data

4.1.1. Properties of the simulated signals

First, the competitive methods were compared on simulated signals. We generated signals with amplitude A = 325 V, frequency f = 50 Hz, added white noise SNR = 60 dB and added higher harmonics (1 % of 3rd, 5th and 7th). The sampling frequency of the generated signals was 12.8 kHz, which amounted to 256 samples per period. At the beginning of the second signal period a jump (drop) of the amplitude of 10 V occurred – the simulation of the signal being loaded at the measurement of contact voltage. The length of the observed window for simulated signals was computed as described in Section 3.2.; using statistical power analysis we determined $l = diam\ (I_\phi) = 30$, $diam\ (I_\sigma) = 50$ (see Fig. 6, green line, we wanted under 1 % of type I errors, which amounts to 5 errors for signals of 512 samples, thus we selected the length of observed window of 30 samples, where less than 5 errors occur).

4.1.2. Properties of the measurement signals

Next, we give the description of measured signals. The fault leading to the contact voltage was simulated with a resistor, which when loaded caused a drop of voltage and thus resulted in the measured contact voltage. The measurement signals present real problems due to hardware limitations that were not specifically considered in the design of the proposed method. For application to the measured signals the hardware can be used in a higher-performance regime or can be upgraded with more efficient components. Despite this drawback we tested the proposed method on currently available signals to investigate the efficiency and robustness of the proposed method in a more difficult regime of measured signals. The properties of the real signals are:
1. the high SNR, approximately SNR = 60 dB with harmonic distortion;
2. the jump of approximately 10 digits, which equals approximately 8 V (the signal is measured with a 10-digit analog-to-digital converter);
3. the jump occurs at zero crossing;
4. low sampling frequency $f_s = 12.8 kHz$ leading to 256 samples per period.

We observed that the measured signals contain more than just the first three odd higher harmonic components, as was tested for the simulated signal. Because of this, we extended our KF model to six harmonic components (5). In this way we achieved better results for the estimation of the fundamental component, as more of the disturbing higher components were separated in the model of the KF. The number of modeled components was selected as a trade-off between the effect on the increased accuracy of the fundamental component and the computation burden of the increased transition matrix.

The length of the observed window for measured signals was computed as described in Section 3.2., using statistical power analysis we determined $l = diam\ (I_\phi) = 30$, $diam\ (I_\sigma) = 50$ (values are the same as for the simulated signals as the properties of both signals are very similar).

$$\mathbf{x}[k+1] = \mathbf{F}[k]\mathbf{x}[k]$$
$$= diag(F_d[k,1], F_d[k,2], F_d[k,3], F_d[k,4], F_d[k,5], F_d[k,6])\,\mathbf{x}[k]. \tag{5}$$

4.2. Evaluation measures

We compare the self-tuning Kalman filter for multi-harmonic signal (STKFM) method with a similar method that does not consider the higher harmonic components (self-tuning Kalman filter – STKF). This comparison gives us good insight on the improvement of the proposed method for the more difficult case of signals. We tested the proposed method on simulated and measured signals. For every tested signal we executed a statistical power test for the optimal length of the observed window of the innovation vector. This length is then used in the experiment.

We calculated the delay of the jump detection when the estimate is at 10 % of the jump (Δt_1), the drop time to 90 % of the jump (Δt_2) (analogous to the step response of a system) and the accuracy at the end of the jump (Fig. 8).
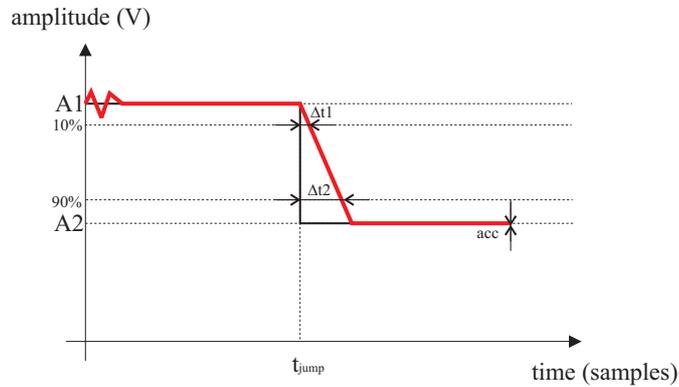

Fig. 8. Illustration of a jump occurring and the notation of the parameters for an interpretation of the results is shown (delay, drop time, accuracy).

The Cramer-Rao lower bound (CRLB) [21] is used in this paper to evaluate the estimation in terms of the theoretical limit of the best performance in terms of estimator variance. We used the well-known equation for the CRLB of the amplitude estimates of the harmonic signals with added white Gaussian noise $CRLB_A = \dfrac{2\sigma^2}{N}$, where σ^2 is the variance of the measurement noise and N is the number of processed samples for the signal [22, 23]. We are aware of the fact that this CRLB is only an approximation since the distribution of the amplitude is not exactly normal. We verified that this CRLB is a conservative assumption and we will not enter into details, but leave it for future work.

5. Experimental results

In this section we present the test results of the proposed Kalman-filter-based method for an amplitude estimation of harmonic signals with added white noise and harmonic distortion (STKFM). The results are given in graphical and tabular form, illustrating the comparison with a competing method. The horizontal axes of the graphs represent the ratio between the number of the current sample (N) and the number of samples for one period (N_p).

5.1. Simulated signals

In this section we present results obtained on simulated signals. Fig.9 shows the tracking of the estimated non-stationary amplitude, in Fig. 10 we give a comparison of variances of STKF and STKFM methods to CRLB, and in Table 1 we show the values of the evaluation measures described in Section 4.2.
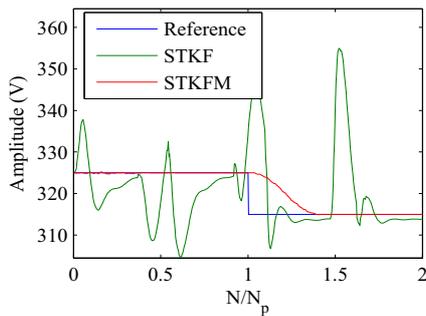

Fig. 9. Amplitude tracking with the proposed STKFM (red) and the competitive STKF (green) at $\Delta A = 10V$, SNR = 60 *db*. Reference amplitude of the signal is the blue line.
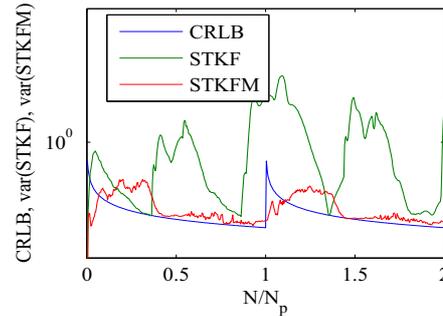
Fig. 10. CRLB (blue), variance of the proposed STKFM (red) and the variance of the competitive STKF (green) $\Delta A = 10V$, SNR = 60 *db*.

Table 1. Evaluation parameters described in Fig. 8 for the amplitude jump of 10 V and SNR of 60 dB.

	Δt_1 (samples)	Δt_2 (samples)	Amplitude (V)
STKFM	11	581	314.9743
STKF	/	/	326.1481
TRUE	0	0	315

Observe that the values of Δt_1 and Δt_2 are zero, as the jump of amplitude is theoretically expected to change in 1 time step.

5.2. Measured signals

In this section we present the results of the proposed method on signals obtained with the real contact-voltage measurement described in Section 2. Fig. 11 and 12 show tracking of the estimated amplitude and comparison of variances to CRLB, respectively.
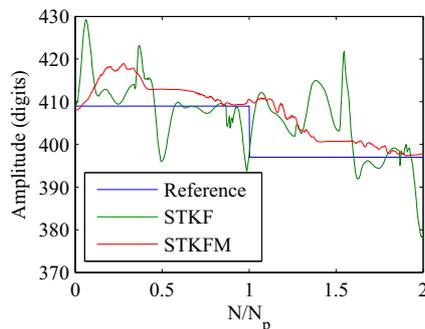

Fig. 11. Amplitude estimation of the real contact-voltage measurement signal with the proposed STKFM (red) and the competitive STKF (green). Reference amplitude of the signal is the blue line.
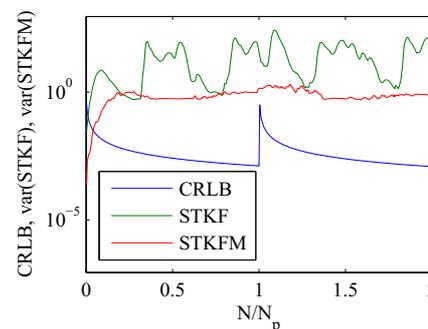
Fig. 12. CRLB (blue), variance of the proposed STKFM (red) and the variance of the competitive STKF (green) depending on the number of processed samples of the real contact-voltage measurement signal.

6. Discussion

6.1. Simulated signals

The results in Fig. 9 show that the proposed STKFM method performs well, as the estimation is fast in adapting to the amplitude jump and accurate in estimating the value of the amplitude. On the other hand, the competitive STKF method does not converge to the estimated amplitude due to the harmonic distortion, which is not considered in the model of KF.

We also present a comparison of both methods' variances to the CRLB in Fig. 10. Again, the proposed method turns out to be more effective than the competitive method.

Finally, we give results of evaluation parameters described in Fig. 8 for the simulated signals in Table 1. It can be observed that the STKF method does not converge to the true value of the new amplitude. The proposed method is, on the other hand, very fast (achieves 90 % of the jump in approximately a quarter of the period; $91 / 256 = 35$ %) and accurate (the estimated amplitude one period after the jump is 314.9724 V; $314.9724 / 315 = 99.99$ %).

6.2. Measured signals

In this section we discuss the results of the proposed method on signals obtained with the real contact-voltage measurement described in Section 2. The results of the amplitude tracking (Fig. 11) show that the proposed method is successful in the described conditions. In comparison with the competing STKF method, the proposed method is more stable and accurate at the end of the period after the amplitude jump occurs. Another problem is the low sampling frequency, but the results show that 256 samples per period are enough for the proposed method to converge to the amplitude of the processed signal. The selected model of the Kalman filter enables us to extend the model to additional higher harmonics and thus the robustness can even be increased. It can be observed from the results that the detection of the jump occurs with a slight delay, which is to be expected as the jump occurs at the worst moment on the signal ($N / N_p = 1$, zero-crossing where the difference between the samples is the largest and so the jump is partially hidden in this difference) and because the use of the confirmation interval n_j for the jump detection is more reliable (Fig. 11).

We also show the comparison of variances of both tested methods with the CRLB (Fig. 12). The variance of the proposed method is mainly lower than the variance of the STKF method, which means that the proposed method is more efficient than the STKF method.

7. Conclusion

The paper presents a new, adaptive, Kalman-filter-based method for estimating the amplitude of noisy harmonic signals with harmonic distortion. The results show that the method can be used for contact-voltage measurements where there are a series of jumps in the amplitude. A statistical power analysis for the configuration of the optimal parameters of the statistical testing was carried out and different experiments were executed for the determination of optimal Kalman-filter parameters. In future work we see new options for research relating to Kalman-filter models for other parameters of the harmonic signals. We will also test other jump detectors and research the ability of the response to jump with the excitation vector. A Kalman filter for non-coherent sampling will be tested as the adaptive property of the filter enables us to use variable transition and measurement matrices.

Acknowledgements

References

[1] Metrel (2008). *Guide for testing and verification of low voltage installations.*

[2] Lušin, T., Agrež, D. (2011). Estimation of the Amplitude Square Using the Interpolated Discrete Fourier Transform. *Metrol. Meas. Syst.*, 18(4), 583–596.

[3] Proakis, J., Manolakis, D. (2006). *Digital Signal Processing.* 4th ed., Prentice Hall.

[4] Poularikas, A. (2006). *Signals and Systems Primer with MATLAB.* 1. CRC Press.

[5] Oppenheim, A., Shafer, R. (1975). *Digital Signal Processing.* Prentice Hall New Jersey.

[6] Stoica, P., Li, H., Li, J. (2000). Amplitude estimation of sinusoidal signals: survey, new results, and an application. *IEEE Transactions on Signal Processing*, 48, 338–352.

[7] Ogunfunmi, A. Peterson, A. (1989). Adaptive methods for estimating amplitudes and frequencies of narrowband signals. *IEEE International Symposium on Circuits and Systems*, 3, 2124–2127.

[8] Caciotta, M., Carbone, P. (1996). Estimation of non-stationary sinewave amplitude via competitive Kalman filtering. *Instrumentation and Measurement Technology Conference, IMTC-96. Conference Proc.. Quality Measurements: The Indispensable Bridge between Theory and Reality, IEEE.*

[9] Dash, P., Jena, R., Panda, G., Routray, A. (2000). An extended complex Kalman filter for frequency measurement of distorted signals. *IEEE Transactions on Instrumentation and Measurement*, 49, 746–753.

[10] Chen, C., Chang, G., Hong, R., Li, H. (2000). Extended real model of Kalman filter for time-varying harmonics estimation. *IEEE Transactions on Power Delivery*, 25, 17–26.

[11] Liu, S. (1998). An adaptive Kalman filter for dynamic estimation of harmonic signals. *In Proc. of 8th International Conference on Harmonics And Quality of Power*, 2, 636–640.

[12] Metrel (2006). *Measurements on electric installations in theory and practice.*

[13] Electrical safety in low voltage distribution systems up to 1000 V a.c. and 1500 V d.c. – Equipment for testing, measuring or monitoring of protective measures – Part 3: Loop impedance (2007). IEC Std. 61557-3.

[14] Chen, C.I., Chang, G.W., Hong, R.C., Li., H.M. (2010). Extended real model of Kalman filter for time-varying harmonics estimation. *IEEE Transactions on Power Delivery*, 25(1), 17–26.

[15] Yu, K., Watson, N., Arrillaga, J. (2005). An adaptive Kalman filter for dynamic harmonic state estimation and harmonic injection tracking. *IEEE Transactions on Power Delivery*, 20, 1577–1584.

[16] Macias, J., Exposito, A. (2006). Self-tuning of Kalman filters for harmonic computation. *IEEE Transactions on Power Delivery*, 21, 501–503.

[17] Wang, J. (2008). Test Statistics in Kalman Filtering. *Journal of Global Positioning Systems*, 7, 81–90.

[18] Miller, R.G.J. (1981). *Simultaneous Statistical Inference.* 2nd ed., Springer Series in Statistics. Springer.

[19] Cohen, J. (1988). *Statistical Power Analysis for the Behavioral Sciences.* 2nd ed., Routledge Academic.

[20] Lehmann, E.L., Romano, J.P. (2010). *Testing Statistical Hypotheses.* Springer Texts in Statistics, Springer.

[21] Soong, T. (2004). *Fundamentals of probability and statistics for engineers.* Wiley.

[22] Rife, D., Boorstyn, R. (1974) Single tone parameter estimation from discrete-time observations. *IEEE Transactions on Information Theory*, 20, 591–598.

[23] Offelli, C., Petri, D. (1992). The influence of windowing on the accuracy of multifrequency signal parameter estimation. *IEEE Transactions on Instrumentation and Measurement*, 41, 256–261.